Interpolation from Lagrange to Holberg

Michel Léger

Abstract. As the order $2n$ tends to infinity, Lagrange interpolators of periodically sampled 1D functions converge to the *sinc* function modulated by two exponentials. One is related to instabilities and the other to Gaussian apodizing. The Hermite interpolation of Lagrange interpolators gives convolutive C^{k+1}-differentiable Lagrange-Hermite interpolators. Whereas their support has width of order $2n+2$, the active part of their impulse response is width of order $\sqrt{2n}$, instead of $2n$ for Holberg interpolators, which are optimal combinations of Lagrange-Hermite interpolators, and therefore much more efficient. Efficient filters can be derived from these differentiable interpolators, as well as numerical schemes of derivatives at any abscissa.

§1. Introduction

Some applications require very large 2D or 3D regular grids, such as finite-difference modeling of seismic waves, for instance. The processing of these grids involves the computing of numerical schemes of first or second derivatives, and also interpolators and filters. These quantities need to be evaluated very efficiently because the requirements in terms of computation time and memory use are critical.

Numerical schemes, interpolators and filters are interrelated issues, and I choose to study them from the viewpoint of interpolation, which is the most general. For sake of simplicity, I assume 1D interpolation of periodically sampled functions, with unit-sampling rate and even orders.

§2. Lagrange Interpolators

Definition 1. *For some function f with known values f_i at abscissae $x_i = i$, $i \in [-n, n]$, the Lagrange interpolator* ([9,6,2,3]) *of order $2n$ is*

$$\mathcal{L}^0_{2n}(\{f_k\}_{k=-n}^{n}, x) = \sum_{i=-n}^{n} f_i \prod_{\substack{j=-n \\ j\neq i}}^{n} \frac{x-j}{i-j} = \sum_{i=-n}^{n} f_i \, p^L_{2n,i}(x). \tag{1}$$

Curve and Surface Fitting: Saint-Malo 1999
Albert Cohen, Christophe Rabut, and Larry L. Schumaker (eds.), pp. 281–290.

ISBN 0-8265-1357-3.

It can be shifted and centered at any integral abscissa i:

$$\mathcal{L}_{2n}^{i}(\{f_k\}_{k=i-n}^{i+n}, x) = \sum_{j=-n}^{n} f_{i+j}\, p_{2n,\,j}^{L}(x-i).$$

Proposition 2. *As $2n \to \infty$, Lagrange polynomials converge to the* sinc *function modulated by two exponentials:*

$$p_{2n,\,i}^{L}(x) = \frac{\sin \pi(x-i)}{\pi(x-i)} \exp\left(\frac{x^2}{n+\frac{1}{2}}\right) \exp\left(\frac{-i^2}{n+\frac{1}{2}}\right) (1 + O(n^{-3})). \tag{2}$$

Proof: Simple changes in (1) give

$$p_{2n,\,i}^{L}(x) = \frac{(-1)^{2n-i}(n!)^2 x}{(n+i)!\,(n-i)!\,(x-i)} \prod_{j=1}^{n}\left(1 - \frac{x^2}{j^2}\right). \tag{3}$$

Since $\prod_{j=1}^{\infty}(1-\frac{x^2}{j^2}) = \frac{\sin(\pi x)}{\pi x}$, we have

$$\prod_{j=1}^{n}\left(1-\frac{x^2}{j^2}\right) = \frac{\sin(\pi x)}{\pi x} \Big/ \prod_{j=n+1}^{\infty}\left(1-\frac{x^2}{j^2}\right). \tag{4}$$

Since $\ln \prod_{j=n+1}^{\infty}(1-\frac{x^2}{j^2}) = -x^2 \sum_{n+1}^{\infty}(\frac{1}{j^2} + O(j^{-4}))$, and since $\frac{1}{j^2} = O(j^{-4}) + \int_{j-1/2}^{j+1/2} \frac{dt}{t^2}$, we obtain

$$\prod_{j=n+1}^{\infty}\left(1-\frac{x^2}{j^2}\right) = \exp\left(-\frac{x^2}{n+\frac{1}{2}} + O(n^{-3})\right). \tag{5}$$

Moreover, by using Stirling formula $n! = n^n \exp(-n)\sqrt{2\pi n}\,(1 + \frac{1}{12n} + \frac{1}{288n^2} + O(n^{-3}))$, and noting that $\ln(1+\frac{1}{12n}+\frac{1}{288n^2}+O(n^{-3})) = \frac{1}{12n}+O(n^{-3})$ and that $\frac{1}{12n}\left(2 - \frac{n}{n+i} - \frac{n}{n-i}\right) = O(n^{-3})$, we obtain $\ln \frac{(n!)^2}{(n+i)!\,(n-i)!} = -(n+i+\frac{1}{2})\ln(1+\frac{i}{n}) - (n-i+\frac{1}{2})\ln(1-\frac{i}{n}) + O(n^{-3})$. Since $\ln(1+x) = x - \frac{x^2}{2} + \frac{x^3}{3} + O(x^4)$, we have $\ln \frac{(n!)^2}{(n+i)!\,(n-i)!} = \frac{-i^2}{n+\frac{1}{2}} + O(n^{-3})$ and hence

$$\frac{(n!)^2}{(n+i)!\,(n-i)!} = \exp\left(\frac{-i^2}{n+\frac{1}{2}} + O(n^{-3})\right). \tag{6}$$

Noting that $(-1)^i \sin \pi x = \sin \pi(x-i)$ and inserting (4), (5) and (6) in (3) concludes the proof. □

According to the first term of (2), Lagrange polynomials converge to the perfect interpolator *sinc* function (Fig. 1). Away from the center of the interval of the data points, the first exponential explains the well-known instabilities (a small change in the data results in a large change in the interpolation), and the second one corresponds to Gaussian apodizing (see *apodization* in [10]), that is, the vanishing effect of the non-centered data points. Note that these two exponentials compensate one another as $x \to i$.

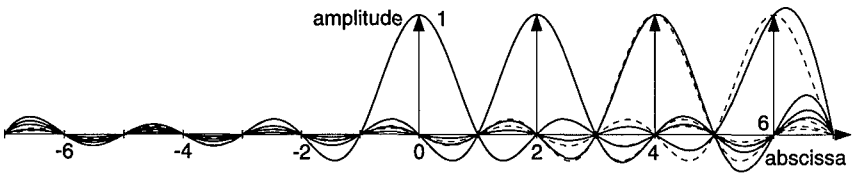

Fig. 1. Lagrange polynomials of order 14 divided by the two exponentials of (2), for $i = 0, 2, 4, 6$. Related *sinc* functions in dotted lines.

§3. Stationary Lagrange Interpolators

Since a Lagrange interpolator is stable only near the middle of the interval of the contributing data points, a natural idea is to change it for each interval between two successive points, in such a way that the interpolator is always used at its best.

Definition 3. *The stationary Lagrange interpolator of order $2n$ uses at abscissa x the Lagrange interpolator of order $2n$ centered at i_x, with $x = i_x + d_x$, $i_x \in \mathbb{N}$, $d_x \in [0, 1[$:*

$$\mathcal{L}_{2n}(\{f_k\}_{k\in\mathbb{Z}}, x) = \sum_{j=-n}^{n} f_{i_x+j}\, p^L_{2n,j}(d_x) = \mathcal{L}^{i_x}_{2n}(x). \tag{7}$$

Remark 4. *Any interpolator such that $\mathcal{I}(\{f_k\}_{k\in\mathbb{Z}}, x) = \sum_{j=a}^{b} f_{i_x+j}\, p_j(d_x)$, with a, b and p_j independent of i_x, is convolutive, that is, there exists a continuous function $\lambda(x)$ such that $\mathcal{I}(\{f_k\}_{k\in\mathbb{Z}}, x) = \Delta(f) * \lambda(x)$, with $\Delta(f) = \sum_{i\in\mathbb{Z}} f_i\, \delta(x-i)$ being the "Dirac comb" modulated by function f.*

This is obvious by considering the impulse response $\lambda(x) = \mathcal{I}(\{\delta_{k0}\}_{k\in\mathbb{Z}}, x) = p_{-i_x}(d_x)$, with δ_{k0} the Kronecker's symbol.

As a particular consequence, stationary Lagrange interpolators are convolutive with impulse responses $\lambda_{2n}(x) = p^L_{2n,\,-i_x}(d_x)$. Moreover, they are also subject to Gaussian apodizing since, as $2n \to \infty$,

$$\lambda_{2n}(x) \sim \frac{\sin \pi x}{\pi x} \exp\left(\frac{-x^2}{n + \frac{1}{2}}\right). \tag{8}$$

It is clear from Fig. 2 that these impulse responses vanish very rapidly as compared to the *sinc* function.

Remark 5. *Since $\forall k,\ k \in [1, 2n]$, $\int_{-\infty}^{+\infty} x^k \lambda_{2n}(x)dx = 0$, then, with $\mathcal{F}$ denoting the Fourier transform, $\forall k,\ k \in [1, 2n]$, $(\mathcal{F}(\lambda_{2n})(u))^{(k)}_{u=0} = 0$ ([1]).*

Hence, stationary Lagrange interpolators are good at low frequencies.

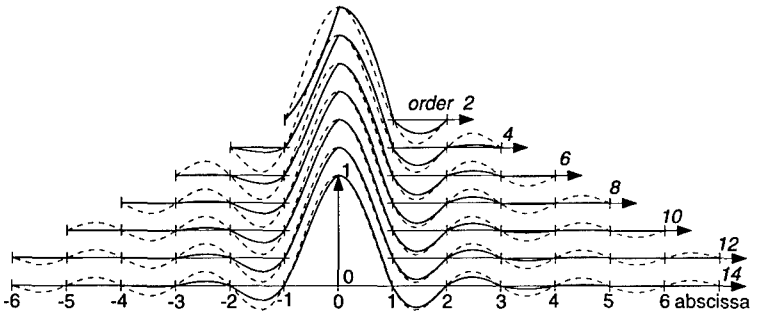

Fig. 2. Impulse responses of stationary Lagrange interpolators for orders 2 to 14 (the last one is truncated). *sinc* function in dotted lines.

§4. Hermite Interpolators

In a general way, Hermite interpolators are consistent with the values of a function and its k (or k_i, $1 \leq i \leq l$) first derivatives at l distinct points [4,2,3]. Here, I consider convolutive interpolators for any k and $l = 2$.

Definition 6. *The C^k piecewise polynomial Hermite interpolator is*

$$\mathcal{H}_k(f) = \Delta(f) * \eta_{k0} + \ldots + \Delta(f^{(j)}) * \eta_{kj} + \ldots + \Delta(f^{(k)}) * \eta_{kk},$$

where $\eta_{kj}(x)$ are $[-1, +1]$-supported basis functions such that $\forall m$, $m \in [0, k]$, $\eta_{kj}^{(m)}(-1) = 0 = \eta_{kj}^{(m)}(+1)$, and $\eta_{kj}^{(m)}(0) = \delta_{mj}$.

From now on, I consider $\eta_{k0}(x)$ functions only.

Proposition 7. *The polynomial expression of Hermite interpolators η_{k0} is*

$$1 - \eta_{k0}(x) = (2k+1)\, C_{2k}^{k} \sum_{j=k}^{j=2k} \frac{(-1)^{j-k} C_k^{j-k}}{j+1}\, x^{j+1} \tag{9}$$

for $x \in [0, 1]$, and $\eta_{k0}(x) = \eta_{k0}(-x)$ for $x \in [-1, 0]$. Moreover, asymptotically,

$$\lim \eta_{k0}(x) \sim \sqcap_0^1(x) * 2\sqrt{\frac{k}{\pi}} \exp(-4kx^2), \quad \textit{when} \quad k \to \infty, \tag{10}$$

with $\sqcap_a^b(x) = 1$ if $x \in [a - \frac{b}{2}, a + \frac{b}{2}]$ and $\sqcap_a^b(x) = 0$ otherwise.

Proof: For $x \in [0, 1]$, it is clear from Def. 6 that $(1-\eta_{k0}(x))^{(1)} = \alpha x^k (1-x)^k$. Since $\eta_{k0}(0) = 1$ and $\eta_{k0}(1) = 0$, we have

$$\frac{1}{\alpha} = \int_0^1 (1 - \eta_{k0}(x))^{(1)} dx. \tag{11}$$

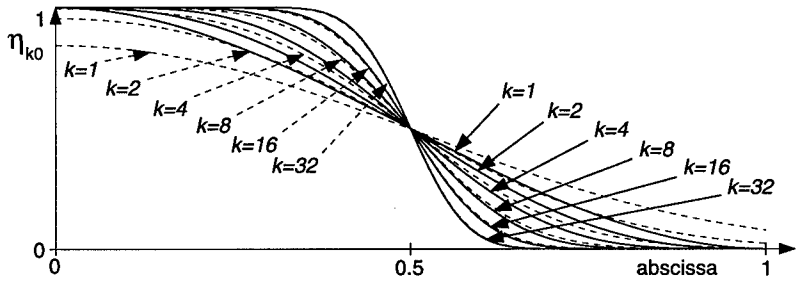

Fig. 3. Right part of impulse responses of Hermite interpolators according to (9), their asymptotic form according (10) in dotted lines.

Let us define $I_{k,l} = \int_0^1 x^k(1-x)^l dx$. Integrating by parts gives $I_{k,l} = \frac{l}{k+1} I_{k+1,l-1}$, that is, $I_{k,k} = \frac{(k!)^2}{(2k)!} I_{2k,0} = C_{2k}^k I_{2k,0}$ by recurrence. Since $I_{2k,0} = \frac{1}{2k+1}$, we obtain $\alpha = (2k+1)C_{2k}^k$, and therefore, from (11),

$$(1-\eta_{k0}(x))^{(1)} = (2k+1)\, C_{2k}^k\, x^k(1-x)^k. \tag{12}$$

The binomial theorem and a simple integration concludes the proof of (9). Moreover, by the change of variable $x = \frac{1}{2}+u$ in (12), we have $-\eta_{k0}^{(1)}(\frac{1}{2}+u) = (2k+1)\, C_{2k}^k\, 4^{-k}\,(1-4u^2)^k$. For any abscissa $u_1 > 0$ we may define $u_k = \frac{u_1}{\sqrt{k}}$ and we have $\exp(-4ku_k^2) = \exp(-4u_1^2)$ and $(1-4u_k^2)^k = (1-4\frac{u_1^2}{k})^k$. Since $\lim_{k\to\infty}(1-4\frac{u_1^2}{k})^k = \exp(-4u_1^2)$, then $(1-4u^2)^k \sim \exp(-4ku^2)$ as $k \to \infty$. Moreover, by using $C_{2k}^k = \frac{(2k)!}{(k!)^2}$ and Stirling formula, we obtain, as $k \to \infty$, $(2k+1)C_{2k}^k 4^{-k} \sim 2\sqrt{\frac{k}{\pi}}$, and then $-\eta_{k0}^{(1)}(x) \sim 2\sqrt{\frac{k}{\pi}}\exp(-4k(x-\frac{1}{2})^2)$. Symmetrically, we have $\eta_{k0}^{(1)}(x) \sim 2\sqrt{\frac{k}{\pi}}\exp(-4k(x+\frac{1}{2})^2)$ for $x \in [-1,0]$. Therefore, $\eta_{k0}^{(1)}(x) \sim 2\sqrt{\frac{k}{\pi}}\exp(-4kx^2) * (\delta(x+\frac{1}{2}) - \delta(x-\frac{1}{2}))$, which concludes the proof of (10) since $\Gamma_0^{1(1)}(x) = \delta(x+\frac{1}{2}) - \delta(x-\frac{1}{2})$. □

Note that Lagrange and Hermite interpolators could be considered as Fourier pairs since the right members of (8) and (10) are mutual Fourier transforms if $\pi^2 n = 4k$.

§5. Lagrange-Hermite Interpolators

Since stationary Lagrange interpolators are good at low frequencies and since Hermite interpolators are differentiable, hence good at high frequencies, combining them is a natural idea.

Definition 8. *For $k \geq 0$, the* Lagrange-Hermite interpolator of order $2n$ *is the smooth Hermite interpolation of two successive Lagrange interpolators, that is,*

$$\mathcal{M}_{2n}^{k+1}(x) = \eta_{k0}(x-i_x)\,\mathcal{L}_{2n}^{i_x}(x) + (1-\eta_{k0}(x-i_x))\,\mathcal{L}_{2n}^{i_x+1}(x).$$

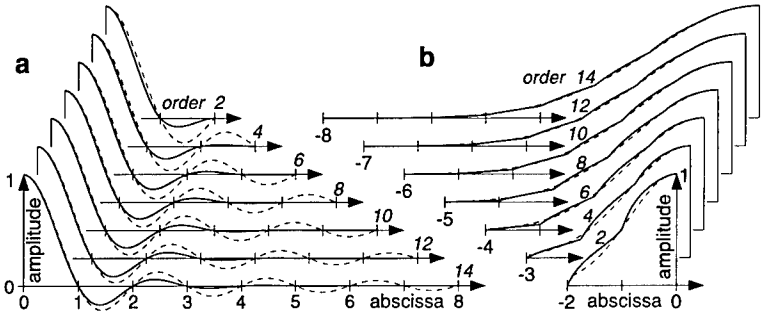

Fig. 4. Right part of the impulse responses of $\mathcal{C}^1$-differentiable Lagrange-Hermite interpolators (**a**), *sinc* in dotted lines. Their left part divided by the *sinc* (**b**), as compared to Gaussian curves $\exp(\frac{-x^2}{n+1/2})$, in dotted lines.

Proposition 9. *For $k \geq 0$, Lagrange-Hermite interpolators $\mathcal{M}_{2n}^{k+1}$ are $\mathcal{C}^{k+1}$-differentiable.*

Proof: Since it is piecewise polynomial, $\mathcal{M}_{2n}^{k+1}$ is $\mathcal{C}^\infty$-differentiable for all non-integral abscissas x. Moreover, $\mathcal{M}_{2n}^{k+1}$ is convolutive, and thus it is sufficient to examine it around $x = 0$. From Def. 8, for $x > 0$, we have $\mathcal{M}_{2n}^{k+1} = \eta_{k0}\,\mathcal{L}_{2n}^0 + (1-\eta_{k0})\,\mathcal{L}_{2n}^1$. From (12), we have $\eta_{k0}(x) = 1 - O(x^{k+1})$, and then $\mathcal{M}_{2n}^{k+1}(x) = \mathcal{L}_{2n}^0(x) + O(x^{k+1})\,(\mathcal{L}_{2n}^1 - \mathcal{L}_{2n}^0)$. Since the interpolators $\mathcal{L}_{2n}^0$ and $\mathcal{L}_{2n}^1$ are continuous, $\mathcal{L}_{2n}^1 - \mathcal{L}_{2n}^0 = O(x)$ and thus $\mathcal{M}_{2n}^{k+1} = \mathcal{L}_{2n}^0 + O(x^{k+2})$. Therefore, for any $j \in [1, k+1]$, $\mathcal{M}_{2n}^{k+1\,(j)}(0^+) = \mathcal{L}_{2n}^{0\,(j)}(0^+)$. The same argument with $\mathcal{M}_{2n}^{k+1} = \eta_{k0}\,\mathcal{L}_{2n}^{-1} + (1-\eta_{k0})\,\mathcal{L}_{2n}^0$ for $x < 0$ leads to $\mathcal{M}_{2n}^{k+1\,(j)}(0^-) = \mathcal{L}_{2n}^{0\,(j)}(0^-)$, which concludes the proof since $\mathcal{L}_{2n}^0(x)$ is a polynomial. □

The Fourier transform of Lagrange-Hermite impulse responses (which I call μ_{2n}^k for interpolator $\mathcal{M}_{2n}^k$) are very similar to those of stationary Lagrange interpolators below the sampling frequency. Beyond the sampling frequency, for the orders 2 to 14, the rejection in dB of the greatest secondary lobe is 27, 30, 32, 33, 34, 35 and 35 in the $\mathcal{C}^0$ case, 42, 47, 51, 53, 55, 57 and 58 in the $\mathcal{C}^1$ case, 33, 36, 37, 38, 39, 40 and 41 in the $\mathcal{C}^2$ case, and slowly decreases for higher differentiabilities. From this viewpoint, the $\mathcal{C}^1$ Lagrange-Hermite interpolators are the best choice.

§6. Holberg Interpolators

Lagrange-Hermite interpolators are good at low and high frequencies, but unsatisfactory inbetween. Indeed, Gaussian apodizing makes λ_{2n} as well as μ_{2n}^k gradually ineffective, since their cost, which is proportional to the length of their support, increases like n, whereas their active part widens like $\sqrt{n}$. Faced with the same problem in terms of numerical schemes, Holberg ([5]) had the idea of combining several orders and optimizing the passband for given tolerance and maximal order. Holberg interpolators just proceed from the same idea.

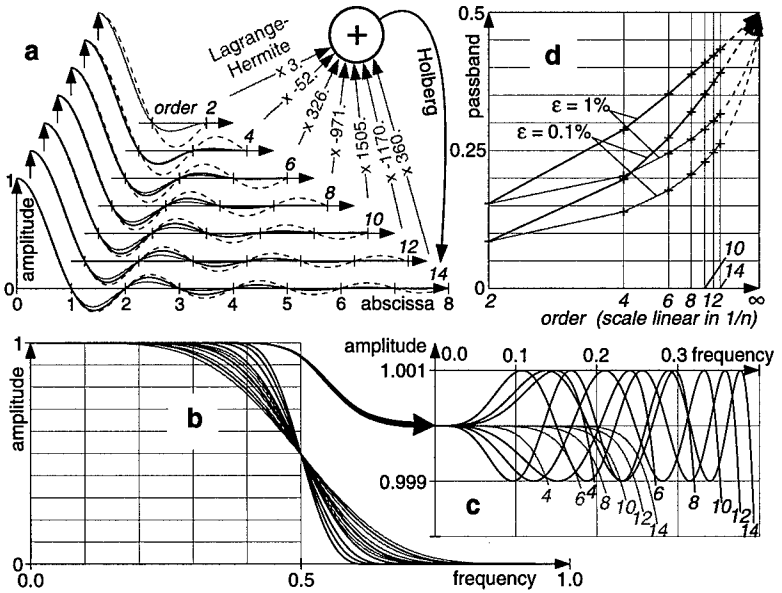

Fig. 5. Impulse responses of $\mathcal{C}^1$-differentiable and 0.1%-precise Holberg interpolators (**a**) (Lagrange-Hermite in grey, *sinc* in dotted lines). Their Fourier transform (**b**) and an enlargement of them (**c**). The passband-*vs*-order diagram (**d**) showing the linear behaviour of Holberg interpolators and the parabolic behaviour of the Lagrange-Hermite interpolators.

Definition 10. *The $2n$-hybrid order, $\mathcal{C}^k$-differentiable and ε-precise Holberg interpolator is the linear combination $\tilde{\mathcal{M}}_{2n}^{k,\varepsilon} = \sum_{i=1}^{i=n} \beta_i^\varepsilon \mathcal{M}_{2i}^k$ such that $\sum_1^n \beta_i^\varepsilon = 1$ and such that the following passband is maximized,*

$$B(\beta_1^\varepsilon, \ldots, \beta_{n-1}^\varepsilon) = \sup(\{\nu;\, \forall \xi \leq \nu;\, |\sum_i \beta_i^\varepsilon \mathcal{F}(\mu_{2i}^k)(\xi) - 1| \leq \varepsilon\}).$$

Clearly, these Holberg interpolators are convolutive, with impulse responses $\tilde{\mu}_{2n}^{k,\varepsilon} = \sum_1^n \beta_i^\varepsilon \mu_{2n}^k$.

Fig. 5 illustrates the case of $\varepsilon = 0.1\%$ and $k = 1$ ($\mathcal{C}^1$-differentiability). Fig. 5a shows that the impulse responses of Holberg interpolators decrease much slower than the Lagrange-Hermite interpolators. The sum of the β_i^ε is one, but their absolute sum may be far from one, for instance about 4300 in the case of the 14th order. In the Fourier domain, Fig. 5b, together with its enlargement Fig. 5c, shows that the passband is increased a lot from Lagrange-Hermite to Holberg.

For tolerances 1% and 0.1%, Fig. 5d shows the *parabolic* behaviour around infinite order of the passbands of the Lagrange-Hermite interpolators (grey arrows are parabolas with vertical tangent at the corner). This is due to Gaussian apodizing, since the Fourier transform of (8) gives the convolution of a box function with a Gaussian function that narrows like $\frac{1}{\sqrt{n}}$ as $n \to \infty$.

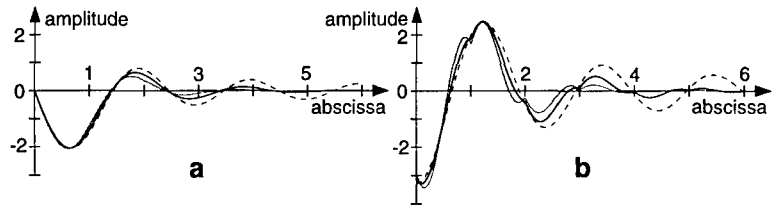

Fig. 6. Right part of the impulse responses of the 10th-order Lagrange-Hermite (in grey) and Holberg interpolators of first (**a**) and second (**b**) derivatives. Perfect (but truncated) interpolators for derivatives are displayed in dotted lines.

On the contrary, the passbands of the Holberg interpolators have a *linear* behaviour (black arrows are straight), which is the best possible one because the active part of the impulse response of the interpolator cannot expand faster than its support. The passbands are referred to the sampling frequency.

The optimization of passband B in the β_i^ε space is difficult because B is discontinuous along $n-1$ hypersurfaces (related to tangencies at $1 \pm \varepsilon$) which intersect at the optimum. To overcome this difficulty, I used a method consisting of the following steps:

1) choose a strictly increasing sequence of frequencies ν_i in $]0, 0.5[$, with $1 \leq i \leq n-1$,
2) set at $1+\varepsilon$ the value of the combination at frequency ν_{n-1}, $1-\varepsilon$ at ν_{n-2}, $1+\varepsilon$ at ν_{n-3}, and so on until ν_1, and finally 1 at frequency $\nu_0 = 0$,
3) solve the linear system for the β_i^ε,
4) detect the frequencies at which the combination is extremal,
5) if these frequencies are close to the ν_i, then stop, else update the ν_i and come back to step 2.

A priori, the feasability of steps 3 and 4 and the convergence are not guaranteed. In practice however, this method works simply well, with less than ten iterations. See also [7,8] on optimal filtering.

§7. Applications

The main application of Holberg interpolators are Holberg numerical schemes ([5]) because they are cost-effective in the field of numerical simulation of acoustic wave propagation. Especially in 3D, this effectiveness is of considerable importance because of the huge amount of computing time needed.

From a $2n$-order $\mathcal{C}^k$-differentiable Lagrange-Hermite or Holberg interpolator, $2n$-order $\mathcal{C}^{k-m}$-differentiable interpolators of the mth derivative ($m \leq k$) can be easily derived, as well as numerical schemes of these derivatives at any abscissa. Fig. 6 shows the responses of the 10th-order Lagrange-Hermite and Holberg ($\varepsilon = 0.1\%$) interpolators of first (a) and second (b) derivatives. The values at integral abscissas give standard numerical schemes. In a similar way, the integration of these impulse responses could result in Newton-Cotes-like Holberg formulas (see *Newton-Cotes Formulas* in [10]).

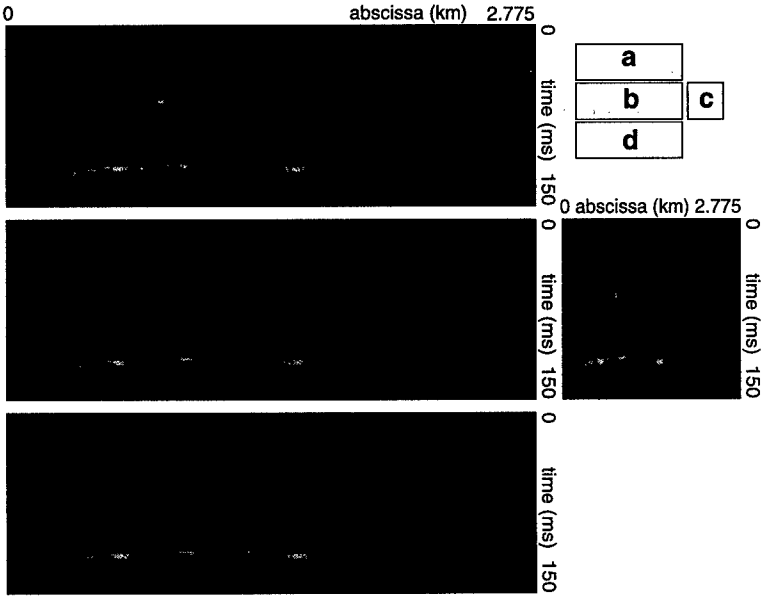

Fig. 7. A seismic section (**a**) has been horizontally filtered (**b**) for antialiasing, threefold undersampled (**c**), and finally interpolated (**d**).

Holberg interpolators, and numerical filters that can be generated from them, are also interesting for their efficiency. For instance, the response of a 1%-precise, 6th-order, $\mathcal{C}^1$ Holberg interpolator has been fourfold oversampled and used to filter horizontally Fig. 7a into Fig. 7b for antialiasing. The threefold undersampling of Fig. 7b gives Fig. 7c. The 1%-precise, 6th-order, $\mathcal{C}^1$ threefold Holberg interpolation of Fig. 7c gives Fig. 7d. The similarity of (**b**) and (**d**) measures the quality of the filtering and of the interpolation.

§8. Conclusions

In the case of periodic data points, Lagrange interpolators converge to a *sinc* function multiplied by two exponentials. The first one explains the well-known instabilities of Lagrange polynomials, which only vanish at the center of the interval of the data points. The second exponential explains the vanishing influence of non-centered data points (Gaussian apodizing). Stationary Lagrange interpolators are stable and convolutive. Hermite interpolators are as differentiable as desired and convolutive and their impulse response converges to the convolution of a box function with a Gaussian function. Lagrange-Hermite interpolators combine the advantages of unlimited order and differentiability. Because of Gaussian apodizing, these interpolators become ineffective at high orders. On the other hand, Holberg interpolators have a much better quality/cost ratio since they are optimal combinations of Lagrange-Hermite interpolators. From Holberg interpolators, efficient numer-

ical schemes of derivatives can be evaluated at any abscissa, and oversampling their impulse response gives short but efficient filters.

Acknowledgments. I would like to thank my colleagues J. Brac, F. Coppens, L. Grizon, E. Maffiolo, L. Nicolétis, J. Pirot and T. Tonellot for their suggestions and many fruitful discussions.

References

1. Bracewell, R., *The Fourier Transform and its Applications*, McGraw-Hill, New-York, 1965.
2. Burden, R. L. and J. D. Faires, *Numerical Analysis*, 3rd edition, PWS Publishers, Boston, 1985.
3. DeVore, R. A. and G. G. Lorentz, *Constructive Approximation*, Springer-Verlag, Berlin, 1993.
4. Hermite, C., Sur la formule d'interpolation de Lagrange. Journal für die reine und angewandte Mathematik **84** (1878), 70–79.
5. Holberg, O., Computational aspects of the choice of operator and sampling interval for numerical differentiation in large-scale simulation of wave phenomena. Geophysical Prospecting **35** (1987), 629–655.
6. Lancaster, P. and K. Šalkauskas, *Curve and Surface Fitting, an Introduction*, Academic Press, London, 1986.
7. McClellan, J. H., T. W. Parks and L. R. Rabiner, A computer program for designing optimum FIR linear phase digital filters. IEEE Transactions on Audio and Electroacoustics **AU-21** (1973) 506–526.
8. Oppenheim, A. V. and R. W. Shafer, *Digital Signal Processing*, Prentice-hall, Englewood Cliffs, New Jersey, 1975.
9. Waring, E., Problems concerning interpolations, Philosophical Transactions of the Royal Society of London **69** (1779), 59–67.
10. Weisstein, E. W., *CRC Concise Encyclopedia of Mathematics*, CRC Press, Boca Raton, 1999.

Michel Léger
1 & 4 avenue de Bois-Préau
92852 Rueil-Malmaison, France
michel.leger@ifp.fr